Nanoscale

Accepted Manuscript

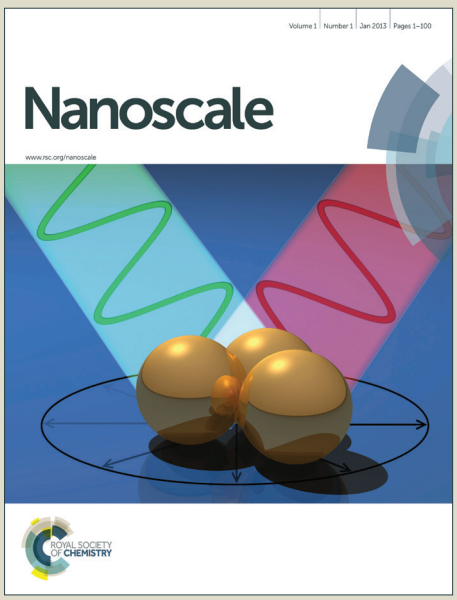

ROYAL SOCIETY OF CHEMISTRY

www.rsc.org/nanoscale

Nanoscale

RSCPublishing

ARTICLE

Reversible Photoswitching Conjugated Polymer Nanoparticles for Cell and *Ex Vivo* Tumor Imaging

Cite this: DOI: 10.1039/x0xx00000x

Guangxue Feng,[ab] Dan Ding,[a] Kai Li,[c] Jie Liu,[a] Bin Liu[ac]*

Received 00th January 2012,
Accepted 00th January 2012

DOI: 10.1039/x0xx00000x

www.rsc.org/

Fluorescent photoswitchable conjugated polymer nanoparticles (PCPNPs) bearing poly(9,9-dihexylfluorene-alt-2,1,3-benzoxadiazole) (PFBD) as the fluorescent host polymer and the photochromic diarylethene as toggle are synthesized via a modified nano-precipitation method using 1,2-distearoyl-sn-glycero-3-phosphoethanolamine-N-[amino(polyethylene glycol)-2000] (DSPE-PEG-NH_2) as the encapsulation matrix. The PCPNPs are spherical in shape with diameters around 34 nm. The fluorescence switching processes upon UV and white light illumination are successfully demonstrated with high contrast up to 90-fold, recovery efficiency of 95%, and excellent repeatability in solution. The cationic PCPNPs can be easily internalized into cancer cells, and accumulate in tumor tissues, where the fluorescence photoswitching processes can be used to self-validate the imaging results.

Introduction

Along with the development of chemistry, material and biological science, fluorescence imaging has been serving as an indispensable tool to visualize biological species or processes within cells, tissues or animals.[1, 2] Various classes of fluorescent materials have been developed and employed in bioimaging and other biological applications. However, the presence of high fluorescence background, interference, and diffraction limitation greatly limit their real world applications.[1] The development of fluorescent photoswitchable materials could circumvent these limitations mostly. Fluorescent photoswitchable materials usually possess two states with distinct absorption and emission properties. The conversion between these two states could be photoinduced as a consequence of molecular level structural modifications.[1-9] The combination and comparison of the fluorescence on and off states help to differentiate fluorescence signals, eliminate background noise or autofluorescence, and provide images with high resolution. The techniques have been emerged in optoelectronic devices, ultrahigh density optical data storage, chemical sensing, as well as in fluorescence microscopic technique with super high spatial resolutions.[10-15]

Various types of fluorescent photoswitching probes, including fluorescent proteins,[16, 17] small organic dyes,[10, 18-20] organic quantum dots (QDs),[21-24] and organic nanoparticles (NPs),[25-27] etc. have been reported up to now. Genetically encoded photoswitchable fluorescent proteins do not need exogenous probes for targeting proteins. However, the low fluorescence signal makes them less attractive in bioimaging applications.[10, 28] On the other hand, spiropyrans or diarylethene modified small organic dyes have been widely used in biological imaging, due to their high brightness, good biocompatibility and fast switching process, [20, 29-34] but with the limitation of poor photostability and small Stokes shift.[35, 36] Recently, photoswitchable QDs with narrow and symmetric emission spectra, bright multiple colours and good photostability have shown great advantages over small organic dyes in bioimaging.[21, 37-39] However, the intrinsic heavy metal components make QDs potentially toxic to biological systems. [40, 41] Therefore, a novel class of fluorescent materials that possesses the merits of small organic dyes and QDs, and overcomes these drawbacks are highly desirable.

Conjugated polymers (CPs) are a class of macromolecules with delocalized π-conjugated backbones.[42, 43] The unique structures bestow them with high extinction coefficient and efficient exciton migration.[43-46] The application of CP nanoparticles (NPs) in *in vitro* and *in vivo* biological imaging has been demonstrated by our group and many others, which revealed that CPNPs have high signal readout ability, good photostability and biocompatibility.[36, 47-52]. Recently, CPs have been employed in fluorescence photoswitching by chemically introducing photochromic segments (spiropyrans or diarylethene) to the backbones or side chains of CPs,[53] or physically co-condensing them together into single NPs.[54, 55] However, the chemically synthesized photoswitchable CPNPs (PCPNPs) suffered from low fluorescence on/off contrast in solutions (on/off ratio ≤ 9), and in cells (on/off ratio = 2).[53] While the current precipitation method required large diarylethene to CP mass ratio (≥ 20) in order to achieve the ~20-fold of fluorescence contrast in solution, leading to low CP loading efficiency (less than 5 wt%) and weak fluorescence.[55] The low fluorescence contrast and weak brightness

constrained their applications in the cellular imaging level and, so far rare was reported on background-rich tumor imaging.[56]

In this contribution, we report the synthesis of fluorescent PCPNPs by modified nano-precipitation method, where CPs and diarylethene are encapsulated into the same NPs. The mass ratio of diarylethene and fluorescent CP is optimized, and the resultant PCPNPs exhibited a high fluorescence quenching ratio of 90-fold upon UV illumination, and recovered 95% of its initial fluorescence after white light exposure in water suspension. The fluorescence turn off and on processes can be reversibly switched for over ten cycles. The cell and tumor imaging performance of the cationic PCPNPs were studied, which showed high fluorescence contrast, and their results self-validated the fluorescence photoswitching ability of PCPNPs.

Experimental Section

Materials. Poly(9,9-dihexylfluorene-alt-2,1,3-benzoxadiazole) (PFBD) was synthesized according to literature.[57, 58] 1,2-Bis(2,4-dimethyl-5-phenyl-3-thienyl)-3,3,4,4,5,5-hexafluoro-1-cyclopentene (Diarylethene) was purchased from Tokyo Chemical Industry Co., Ltd.. 1,2-Distearoyl-sn-glycero-3-phosphoethanolamine-N-[amino(polyethylene glycol)-2000] (DSPE-PEG-NH_2) was purchased from Avanti Polar Lipids, Inc.. Fetal bovine serum (FBS) was purchased from Gibco (Lige Technologies, Ag, Switzerland). 3-(4,5-Dimethylthiazol-2-yl)-2,5-diphenyl tetrazolium bromide (MTT), tetrahydrofuran (THF), dimethyl sulfoxide (DMSO)， and penicillin-streptomycin (PS) solution were purchased from Sigma-Aldrich. Dulbecco's modified essential medium (DMEM) was a commercial product of National University Medical Institutes (Singapore). Phosphate-buffer saline (PBS; 10×) buffer with pH 7.4 (ultrapure grade) is a commercial product of first BASE Singapore. Milli-Q Water (18.2MΩ) was used to prepare the buffer solutions from the 10 × PBS stock buffers. PBS (1×) contains NaCl (137 mM), KCl (2.7 mM), Na_2HPO_4 (10 mM) and KH_2PO_4 (1.8 mM).

Characterization. The UV-vis spectra of PCPNP aqueous suspension were recorded on a Shimadzu UV-1700 spectrometer. The fluorescence spectra were measured using a fluorometer (LS-55, Perkin Elmer, USA). The zeta potential of PCPNPs in aqueous suspension was measured using a Brookhaven ZetaPlus zeta-potential analyser at room temperature. The average particle size and size distribution of the nanoparticles were determined by laser light scattering with a particle size analyzer (90 Plus, Brookhaven Instruments Co. USA) at a fixed angle of 90° at room temperature. The morphology of PCPNPs was studied by high-resolution transmission electron microscope (HR-TEM, JEM-2010F, JEOL, Japan).

Preparation of Nanoparticles. The PCPNPs were prepared via matrix-encapsulation method. 0.5 mg of DSPE-PEG-NH_2, 0.125 mg of PFBD, 0.125 mg of diarylethene were dissolved in 1 mL of THF solution, and well mixed. The THF mixture was dropwise added into 10 mL of MilliQ water under sonication at 18W output using a microtip probe sonicator (XL2000, Misonix Incorporated, NY). The mixture was stirred at 600 rpm at room temperature overnight for THF evaporation. The PCPNPs were concentrated by water evaporation under Argon flow at 60 °C, and stored at room temperature until further use. To prepare PCPNPs with optimized fluorescence quenching and recovery performance, different PFBD to diarylethene weight ratios were used following the same procedure, while keeping their total amount as 0.25 mg.

Calculation of NP Concentration. Freeze-drying of the PCPNP stock suspension (1.5 mL) yielded 1.83 mg of powders. The density of compact NPs is estimated as ~ 1 g/cm^3. As the average size of PCPNPs determined from HR-TEM is ~ 34 nm, the concentration of the PCPNPs in stock can be calculated from the following equation:
Total number of PCPNPs in 1.5 mL solution:

$$N = \frac{\frac{1.83 \times 10^{-3} g}{1\ g/mL}}{\frac{1}{6}\pi \times 34^3 \times 10^{-21}\ mL} = 8.9 \times 10^{13}$$

PCPNPs concentration:

$$C = \frac{\frac{8.9 \times 10^{13}}{6.02 \times 10^{23}\ /mol}}{1.5 \times 10^{-3} L} = 98\ nM$$

Cell Culture. Mouse C6 glial cells and human embryonic kidney 293T cells were cultured in DMEM containing 10% fetal bovine serum and 1% penicillin streptomycin at 37 °C in a humidified environment containing 5% CO_2. Before the experiment, the cells were pre-cultured until confluence was reached.

Cellular Imaging. C6 glial cells were cultured in Chamber (LAB-TEK, Chambered Coverglass System, Rochester, USA) at 37 °C. After 80% confluence, the medium was removed, and the adherent cells were washed twice with 1×PBS buffer. PCPNPs (2 nM) in cell culture medium were then added to the chamber. After incubation for 4 h at 37 °C, the cells were washed twice with 1× PBS buffer and then fixed by 75% ethanol for 20 min at 37 ℃, and further washed twice with 1 ×PBS buffer. The sample was imaged by confocal laser scanning microscopy (CLSM) (Zeiss LSM 410, Jena, Germany) with imaging software (Olympus Fluoview FV1000) with signal obtained above 505 nm upon excitation at 488 nm. For fluorescence switching experiments, the fixed C6 cells were pre-treated with reversible cycle of 254 nm UV lamp and white light exposure before CLSM imaging.

Cytotoxicity of PCPNPs. The metabolic activity of Mouse C6 glial cells and human embryonic kidney 293T cells against PCPNPs was evaluated using methylthiazolyldiphenyltetrazolium bromide (MTT) assays. Mouse C6 glial cells and human embryonic kidney 293T cells were seeded in 96-well plates (Costar, IL, USA) at an intensity of 4 × 10^4 cells/mL. After 48 h incubation, the old medium was replaced by PCPNP suspension in DMEM at concentrations of 2, 4, and 10 nM at 37 ℃ and the cells were further incubated for 48 h, respectively. The wells were then washed with 1× PBS buffer and 100 μL of freshly prepared MTT (0.5 mg/mL) solution in FBS-free culture medium was added into each well. The MTT medium solution was carefully removed after 3 h incubation in the incubator. Filtered DMSO (100 μL) was then added into each well, and the plate was gently shaken for 10 min at room temperature to dissolve all the precipitates formed. The absorbance of MTT at 570 nm was

monitored by a microplate reader (Genios Tecan). Cell viability was expressed by the ratio of the absorbance of the cells incubated with PCPNP to that of the cells incubated with culture medium only, which is arbitrary defined as 100%.

Tumor imaging. All the animal studies were performed in compliance with the guidelines set by The Institutional Animal Care and Use Committee (IACUC). C6 glial cells suspension in 1× PBS containing 3–4×10^6 cells (0.15 mL) was injected subcutaneously to the ICR mice at the left axilla. When the tumour volume reached a mean size of about 300 mm^3, the mouse was intravenously injected with PCPNPs (98 nM, 200 μL). At 24 h post intravenous injection, the tumour bearing mouse was sacrificed, and the liver, spleen, kidney. Heart, lung and tumor were harvested for isolated organ imaging. These organs were imaged using Maestri system (Cri, Inc.). The light with a central wavelength at 453 nm was selected as the excitation source. Ex vivo spectral imaging from 560 to 900 nm (10 nm step) was carried out with an exposure time of 150 ms for each image frame. The auto-fluorescence was removed using spectral unmixing software. The tumor was further cut into sections (6 μm) with a microtomy at –24°C (Leica CM Rapid Sectioning Cryostat) and imaged by CLSM with signal obtained above 505 nm upon excitation at 488 nm.

Results and Discussion

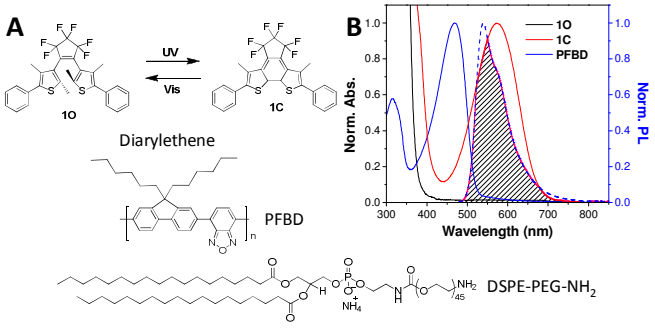

***Scheme 1**. A) Chemical structures of diarylethene, PFBD, and DSPE-PEG-NH_2. B) Absorption spectra of diarylethene and PFBD (solid lines) and emission spectrum of PFBD (dashed line) in THF solution.*

The PCPNPs were prepared *via* a modified nano-precipitation method, where the photo-modulator and fluorescent polymer were encapsulated into the same NP by a block copolymer matrix.[47, 49, 59] In order to achieve the reversible photoswitching performance, a photochromic molecule with high fatigue resistance, diarylethene (Scheme 1A), was selected as the fluorescence modulator. Diarylethene cannot quench the host polymer in its ring open form while it is an efficient quencher in its ring close form (Scheme 1B).[34, 54, 55] The alternation of ring close or open can be reversibly induced by ultra-violet (UV) or visible light irradiation. Poly(9,9-dihexylfluorene-alt-2,1,3-benzoxadiazole) (PFBD)[57, 58] (Scheme 1A) was selected as the fluorescent polymer because its emission spectrum overlaps well with the absorption spectrum of ring-close diarylethene (Scheme 1B), which favours fluorescence quenching *via* energy transfer in the quenched state. In addition, previous studies revealed that PFBD possesses high brightness, good photostability, and compatible excitation wavelength with 488 nm CLSM laser.[58,59] Cationic lipid, 1,2-distearoyl-sn-glycero-3-phosphoethanolamine-N-[amino(polyethylene glycol)-2000] (DSPE-PEG-NH_2) was utilized as the encapsulation matrix due to its good encapsulation performance, high biocompatibility, and rendered cationic charges at the NP surface.[49, 59]

Scheme 2 shows the formation of PCPNPs in water. Briefly, diarylethene, PFBD and DSPE-PEG-NH_2 were dissolved and well mixed in THF solution. The THF mixture was then dropwise added into MilliQ water upon 10-fold dilution under the continuous sonication. Upon dilution, hydrophobic DSPE segment, PFBD and diarylethene intertwine with each other to form the core while hydrophilic PEG-NH_2 segment will render outside toward aqueous phase. The extended PEG chains provide a protective shell layer for the PCPNPs and prevent them from further aggregation. The amino group terminated PEG chains also render the NPs positive surface charge, which benefits cell internalization.[60] THF was subsequently removed under stirring and the PCPNPs was stored at room temperature.

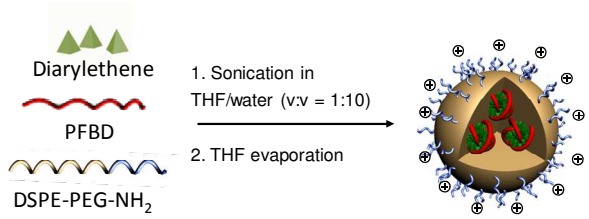

***Scheme 2**. Schematic illustration of PCPNPs formation in aqueous suspension.*

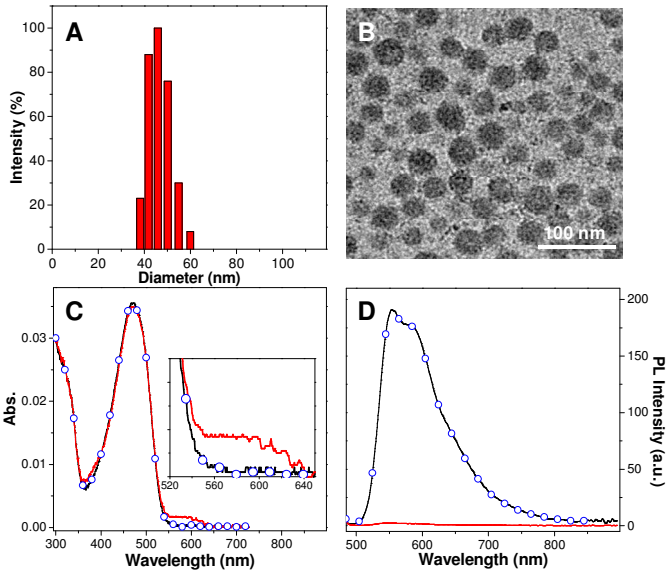

***Figure 1**. A) Laser light scattering, B) transmission electron microscopy of PCPNPs. C) Absorption spectra, and D) emission spectra changes of PCPNPs in aqueous suspension, without any treatment (black line), after treatment with UV irradiation (red line), and after white light illumination (circle).*

The size and morphology of obtained PCPNPs were firstly investigated by laser light scattering (LLS) and transmission electron microscopy (TEM). The LLS result revealed a volume average hydrodynamic diameter ~43±1.2 nm of PCPNPs with unimodal peak and narrow size distribution (Figure 1A). TEM image shows that PCPNPs are uniformly distributed, and in clearly distinguishable spherical shapes with a mean size of ~34±0.8 nm (Figure 1B). The smaller size measured by TEM should be contributed to the NP shrinkage in the dry state, as well as different measurement principles of LLS and TEM, where LLS results take the extended hydrophilic segments into consideration. The surface zeta potential of PCPNPs was measured to be ~18 mV in 1× PBS buffer, which should promote cellular uptake as compared to neutral or negatively charged nanoparticles.[60] It should be noted that the nanoparticles are well dispersed in water, and no precipitation was observed even after being stored at room temperature for three months, indicating good colloidal stability of the cationic PCPNPs.

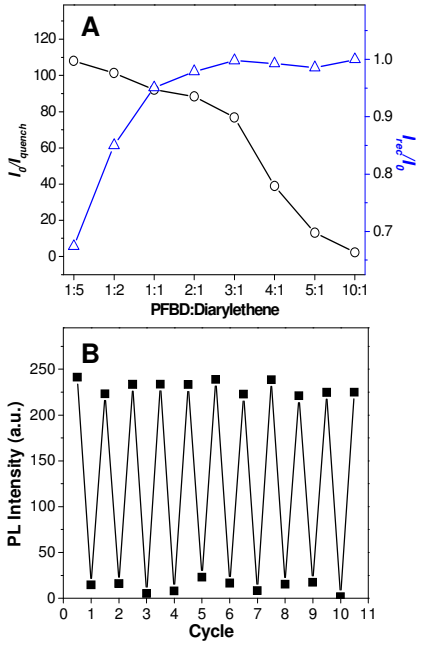

***Figure 2**. A) Fluorescence quenching ratio after UV irradiation (○) and recovery ratio after visible irradiation (Δ) for PCPNPs with different PFBD to diarylethene weight ratios. I_0 is the initial fluorescence, I_{quench} is the fluorescence after 254 nm irradiation, and I_{rec} is the recovered fluorescence after white light exposure. B) Fluorescence changes (■) of PCPNPs (PFBD to diarylethene mass ratio is 1:1) upon various UV and visible light irradiation alterations.*

The optical properties of PCPNPs were subsequently studied. The absorption spectrum of PCPNPs has a peak centred at ~470 nm (Figure 1C), which is attributed to PFBD. After UV irradiation, a smaller shoulder between 540 and 640 nm is observed, which is contributed by diarylethene in its ring open form. Upon treatment with white light, the shoulder disappears, indicating the ring close process of diarylethene. The emission spectrum of PCPNPs centred at ~560 nm (Figure 1D), with a high quantum yield of 30%. The fluorescence is efficiently quenched upon UV irradiation exposure and it fully recovered after white light treatment. The fluorescence quenching reveals efficient energy transfer from PFBD to diarylethene when they are in proximity. The UV and white light irradiations demonstrate that PCPNPs possess the ability of fluorescence switching between on and off states. It should be noted that the fluorescence profiles of PCPNPs are hardly affected after 3 month storage.

Different PFBD to diarylethene ratios were examined to optimize the photoswitching performance of PCPNPs. In the experiment design, the weight of DSPE-PEG-NH_2 is kept as 0.5 mg, while the weights of diarylethene (X mg) and PFBD (Y mg) are varied (X + Y = 0.25). The fluorescence quenching ratios upon 254 nm light exposure and the recovery ratios upon white light exposure are shown in Figure 2A. At the PFBD to diarylethene mass ratio of 1:5, the PCPNPs exhibited an a large quenching ratio over 110-fold, while only 63% of fluorescence can be recovered even after 1 h white light exposure. In the contrary, when the PFBD to diarylethene mass ratio increases to 10:1, the quenching ratio decreases to less than 10-fold, while fluorescence can be fast recovered with approximately 100% efficiency (Figure 2A). As both the quenching and recovery ratios have to be balanced to obtain the overall ideal photoswitching performance, the weight ratio of PFBD to diarylethene is optimized at 1:1, where the fluorescence can be quenched up to 90-fold at dark state and can be recovered to over 95% in the fluorescence state. This contrast ratio is at least 4-fold higher than those reported for other photoswitchable CP systems.[53,55] The high fluorescence contrast and brightness makes PCPNPs promising for tumor imaging. The repeatability of PCPNPs was subsequently assessed by checking the fluorescence intensity change upon several cycles of UV and white light exposure alterations. The result is shown in Figure 2B. The PCPNPs undergo efficient fluorescence quenching and recovery processes for over 10 cycles, indicating good repeatability of the obtained PCPNPs. It should be noted that the fluorescence of PCPNPs can still be recovered even after being pre-treated with 254 nm irradiation for 3 h, suggesting the high photostability. In addition, the dark state of PCPNPs can be reserved for over 48 h without white light exposure, indicating high resistance of the dark state to other external factors other than white light.

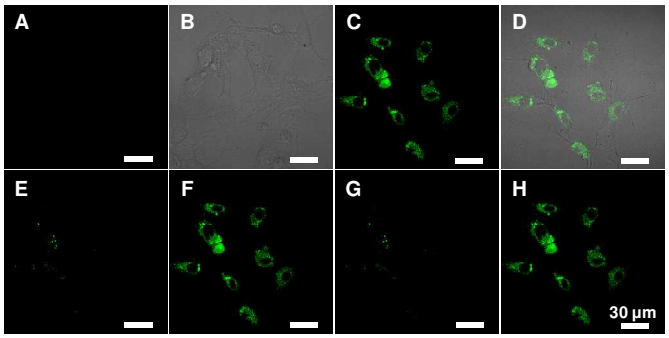

***Figure 3**. A) Fluorescence image, and B) fluorescence/bright field merged image of blank C6 glial cells. C) Fluorescence and D) fluorescence/bright field merged image of C6 glial cells after 4 h incubation with 2 nM PCPNPs at 37 ºC. Fluorescence image of C6 after UV irradiation (E, and G), or visible light irradiation (F and H). The signal is collected above 505 nm upon excitation at 488 nm.*

Inspired by the excellent photoswitching performance of PCPNPs in water suspension, we subsequently applied them in cellular and tumor imaging. The *in vitro* cellular imaging was accessed by CLSM using C6 glial cells as the example cell line. As control, blank C6 cells were firstly imaged, as shown in Figures 3A and B, no fluorescence was observed. Figures 3 C and D show the fluorescence images of C6 cell after treatment with 2 nM PCPNPs for 4 h at 37 ºC, which reveals a bright green fluorescence and clear cell shapes. After UV irradiation, the fluorescence fades out, and negligible signal can be detected (Figures 3E and G), due to the photoinduced ring close process of diarylethene. The white light exposure brings green fluorescence back to the C6 cells (Figures 3F and H), which is consistent with the results shown in Figure 2. The fluorescence intensity of the C6 cells in the fluorescence-on state is 16-fold of that in the dark state. The cellular fluorescence turn off and on processes can be repeated for many cycles, suggesting the high photostability and fluorescence repeatability of PCPNPs inside the cells. The cytotoxicity of PCPNPs against C6 cells and human embryonic kidney 293T cells were also evaluated *via* MTT assay. As shown in Figure 4, the viabilities of C6 and 293T cells remain almost 100% even after 48 h incubation with 10 nM PCPNPs, revealing the low cytotoxicity of PCPNPs.

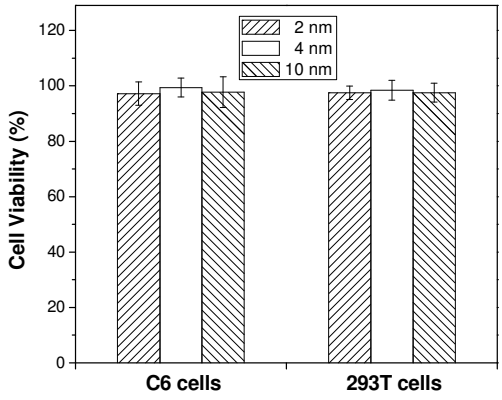

Figure 4. *Cell Viability of mouse C6 glial cells or* human embryonic kidney 293T cells *after 48 h incubation with PCPNPs at 2, 4, 10 nM, respectively. The percentage cell viability of treated cells is calculated relative to that of the untreated cells with a viability arbitrarily defined as 100%.*

The tumor imaging of PCPNPs was studied on a tumor-bearing mouse model. The tumor tissues were obtained via subcutaneously inoculating C6 glial cells into the left axillary space of ICR mouse. PCPNPs (0.2 mL, 98 nM) were intravenously injected to tumor-bearing mouse. At 24 h post-injected, the mouse was sacrificed, and the kidney, spleen, liver, heart, lung and tumor were harvested for isolated organ imaging. Figure 5A showed the *ex vivo* images of these organs. The PCPNPs exhibited tumor targeting ability, where tumor tissue showed higher fluorescence than spleen, kidney, heart, and lung, except for liver. The accumulation of PCPNPs in tumor site should be due to passive targeting through enhanced permeability and retention (EPR) effect, which results from the tumor microenvironment.[61] The accumulation of PCPNPs in liver and kidney should be contributed by reticuloendothelial system (RES) and mononuclear phagocyte system (MPS) uptake.[62,63] The tumor photoswitching experiment was conducted on the tumor section, where the green fluorescence from tumor tissue decreases to a distinguishable level with only one-tenth of fluorescence remained upon UV light treatment (Figures 5B and C). The fluorescence is recovered after white light exposure (Figures 5C and D). This alteration process can be repeated for many cycles ($n \geq 7$) (Figures 5B-G), further indicating the high stability of our PCPNPs in the biological systems. The fluorescence contrast level in the tumor tissue is still over 10-fold, and such a high fluorescence contrast ($\geq$ 11) benefits signal identification, especially in background-rich *in vivo* imaging.

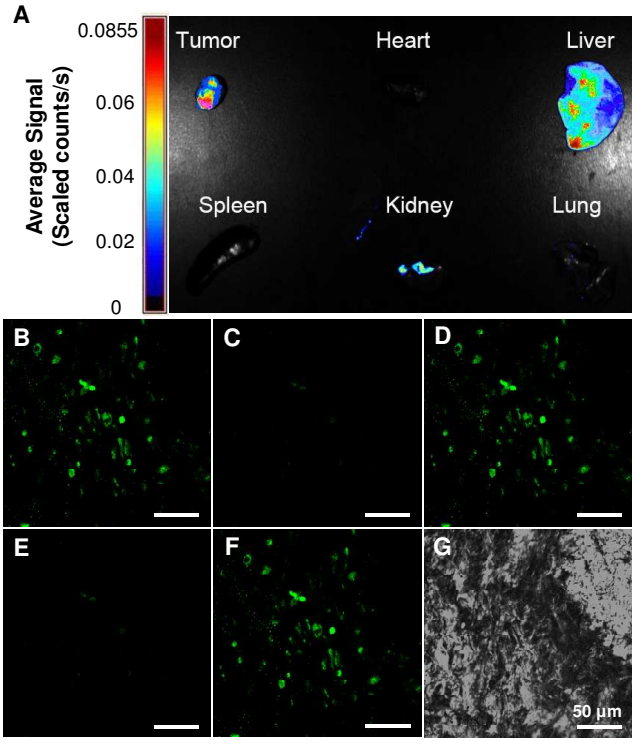

Figure 5. *A) Fluorescence image of different organs at 24 h post-administration. CLSM images of the tumor slice, B), D) and F) after visible light irradiation, C) and E), after UV irradiation, G) bright field imaging. The signal is collected above 505 nm upon excitation at 488 nm.*

Conclusions

In conclusion, we fabricated fluorescence photoswitchable NPs based on conjugated polymers. The green fluorescent PFBD and the photochromic diarylethene are physically blended into a single NP with high colloidal stability. The formed PCPNPs exhibit spherical morphology with an average diameter of ~34 nm, and a high fluorescence quantum yield of 30% in its fluorescence state. The fluorescence switching between on and off state was successfully demonstrated in water suspension with a fluorescence quenching ratio up to ~90-fold, and an almost fully recovery fluorescence ratio of ~95%, which can be repeated for several cycles. Upon treatment with cancer cells or injection into tumor bearing mouse, bright fluorescence is observed in the cytoplasm and tumor tissues, respectively. The photoswitching still can be achieved with a

fluorescence on to off ratio over 10-fold. It should be noted that PCPNPs fabricated by this method is able to render the particle different functional group, available for further functionalization for different purposes. This study of PCPNPs in tumor imaging with high fluorescence contrast should open new opportunities for further development of photoswitching NPs in *in vivo* applications.

Acknowledgements

The authors are grateful to the Singapore National Research Foundation (R279-000-390-281), Singapore Ministry of Defence (R279-000-340-232), SMART (R279-000-378-592), the Economic Development Board (Singapore-Peking-Oxford Research Enterprise, COY-15-EWI-RCFSA/N197-1), and Institute of Materials Research and Engineering of Singapore (IMRE/12-8P1103) for financial support.

Notes

[a] Department of Chemical and Biomolecular Engineering, National University of Singapore, 117576, Singapore.

[b] Environmental Research Institute, National University of Singapore, 117411, Singapore..

[c] Institute of Materials Research and Engineering, 117602, Singapore. .

Received: Month XX, XXXX; Revised: Month XX, XXXX; Published online:

Keywords: ((Conjugated polymers, nanoparticles, photoswitching, cell imaging, tumor imaging))

Reference:

1. Z. Tian and A.D.Q. Li, *Acc. Chem. Res.*, 2013, **46**(2), 269-279.
2. Z. Tian, W. Wu, and A.D.Q. Li, *ChemPhysChem*, 2009, **10**, 2577-2591.
3. M. Fernández-Suárez and A.Y. Ting, *Nat. Rev. Mol. Cell Biol.*, 2008, **9**, 929-943.
4. W. Wu and A.D.Q. Li, *Nanomedicine*, 2007, **2**, 523-531.
5. I. Yildiz, E. Deniz, and F.M. Raymo, *Chem. Soc. Rev.*, 2009, **38**, 1859-1867.
6. M. Bossi, V. Belov, S. Polyakova, and S.W. Hell, *Angew. Chem. Int. Ed.*, 2006, **45**(44), 7462-7465.
7. V. Ferri, M. Scoponi, C.A. Bignozzi, D.S. Tyson, F.N. Castellano, H. Doyle, and G. Redmond, *Nano Lett.*, 2004, **4**(5), 835-839.
8. T. Fukaminato, T. Umemoto, Y. Iwata, S. Yokojima, M. Yoneyama, S. Nakamura, and M. Irie, *J. Am. Chem. Soc.*, 2007, **129**(18), 5932-5938.
9. M. Irie, T. Fukaminato, T. Sasak, N. Tamai, and T. Kawai, *Nature*, 2002, **420**, 759-760.
10. M. Bates, B. Huang, G.T. Dempsey, and X. Zhuang, *Science*, 2007, **317**(5845), 1749-1753.
11. M. Heilemann, S. van de Linde, M. Schüttpelz, R. Kasper, B. Seefeldt, A. Mukherjee, P. Tinnefeld, and M. Sauer, *Angew. Chem. Int. Ed.*, 2008, **47**(33), 6172-6176.
12. B. Huang, W. Wang, M. Bates, and X. Zhuang, *Science*, 2008, **319**(5864), 810-813.
13. S.J. Lord, N.R. Conley, H.-l.D. Lee, R. Samuel, N. Liu, R.J. Twieg, and W.E. Moerner, *J. Am. Chem. Soc.*, 2008. **130**(29), 9204-9205.
14. S.W. Hell, *Nature*, 2003, **21**, 1347-1355.
15. H. Shroff, C.G. Galbraith, J.A. Galbraith, and E. Betzig, *Nat. Methods*, 2008, **5**, 417-423.
16. J.S. Biteen, M.A. Thompson, N.K. Tselentis, G.R. Bowman, L. Shapiro, and W.E. Moernet, *Nat. Methods*, 2008, **5**, 947-949.
17. M. Andresen, A.C. Stiel, J. Fölling, D. Wenzel, A. Schönle, A. Egner, C. Eggeling, S.W. Hell, and S. Jakobs, *Nat. Biotechnol.*, 2008, **26**, 1035-1040.
18. C. Flors, J.-i. Hotta, H. Uji-i, P. Dedecker, R. Ando, H. Mizuno, A. Miyawaki, and J. Hofkens, *J. Am. Chem. Soc.*, 2007, **129**(45), 13970-13977.
19. Y. Zou, T. Yi, S. Xiao, F. Li, C. Li, X. Gao, J. Wu, M. Yu, and C. Huang, *J. Am. Chem. Soc.*, 2008, **130**(47), 15750-15751.
20. Z. Tian, W. Wu, W. Wan, and A.D.Q. Li, *J. Am. Chem. Soc.*, 2009, **131**(12), 4245-4252.
21. W.H. Binder, R. Sachsenhofer, C.J. Straif, and R. Zirbs, *J. Mater. Chem.,* 2007, **17**(20), 2125-2132.
22. I. Yildiz, E. Deniz, and F.M. Raymo, *Chem. Soc. Rev.*, 2009, **38**(7), 1859-1867.
23. F.M. Raymo and M. Tomasulo, *Chem. Soc. Rev.*, 2005, **34**(4), 327-336.
24. S.E. Irvine, T. Staudt, E. Rittweger, J. Engelhardt, and S.W. Hell, *Angew. Chem. Int. Ed.*, 2008. **47**(14), 2685-2688.
25. J. Chen, F. Zeng, S. Wu, Q. Chen, and Z. Tong, *Chem. Eur. J.*, 2008, **14**(16), 4851-4860.
26. L. Zhu, W. Wu, M.-Q. Zhu, J.J. Han, J.K. Hurst, and A.D.Q. Li, *J. Am. Chem. Soc.*, 2007, **129**(12), 3524-3526.
27. M.-Q. Zhu, L. Zhu, J.J. Han, W. Wu, J.K. Hurst, and A.D.Q. Li, *J. Am. Chem. Soc.*, 2006, **128**(13), 4303-4309.
28. H. Shroff, C.G. Galbraith, J.A. Galbraith, H. White, J. Gillette, S. Olenych, M.W. Davidson, and E. Betzig, *Proc. Natl. Acad. Sci. U.S.A.*, 2007, **104**(51), 20308-20313.
29. M.-Q. Zhu, G.-F. Zhang, C. Li, M.P. Aldred, E. Chang, R.A. Drezek, and A.D.Q. Li, *J. Am. Chem. Soc.*, 2009,**133**, 365-372.
30. Z. Tian, W. Wu, W. Wan, and A.D.Q. Li, *J. Am. Chem. Soc.*, 2011, **133**, 16092-16100.
31. J. Chen, P. Zhang, G. Fang, P. Yi, F. Zeng, and S. wu, *J. Phys. Chem. B*, 2012, **116**, 4354-4362.
32. R. Arai, S. Uemura, M. Irie, and K. Matsuda, *J. Am. Chem. Soc.*, 2008, **130**, 9371-9379.
33. T. Fukaminato, T. Doi, N. Tamaoki, K. Okuno, Y. Ishibashi, H. Miyasaka, and M. Irie, *J. Am. Chem. Soc.*, 2011, **133**(13), 4984-4990.
34. S.-C. Pang, H. Hyun, S. Lee, D. Jang, M.J. Lee, S.H. Kang, and K.-H. Ahn, *Chem. Commun.*, 2012, **48**, 3745-3747.
35. U. Resch-Genger, M. Grabolle, S. Cavaliere-Jaricot, R. Nitschke, and T. Nann, *Nat. Methods*, 2008, **5**, 763-775.
36. C. Wu, T. Schneider, M. Zeigler, J. Yu, P.G. Schiro, D.R. Burnham, J.D. McNeill, and D.T. Chiu, *J. Am. Chem. Soc.*, 2010, **132**(43), 15410-15417.
37. S.A. Díaz, G.O. Menéndez, M.H. Etchehon, L. Giordano, T.M. Jovin, and E.A. Jares-Erijman, *ACS Nano*, 2011, **5**(4), 2795-2805.
38. S.A. Díaz, L. Giordano, T.M. Jovin, and E.A. Jares-Erijman, *Nano Lett.*, 2012, **12**(7), 3537-3544.
39. L. Zhu, M.-Q. Zhu, J.K. Hurst, and A.D.Q. Li, *J. Am. Chem. Soc.*, 2005, **127**(25), 8968-8970.
40. B. Dubertret, P. Skourides, D.J. Norris, V. Noireaux, A.H. Brivanlou, and A. Libchaber, *Science*, 2002, **298**(5599), 1759-1762.
41. A.M. Smith, H. Duan, A.M. Mohs, and S. Nie, *Adv. Drug Deliv. Rev.*, 2008, **60**(11), 1226-1240.
42. B. Liu and G.C. Bazan, *Chem. Mater.*, 2004, **16**(23), 4467-4476.
43. D.T. McQuade, A.E. Pullen, and T.M. Swager, *Chem. Rev.*, 2000, **100**(7), 2537-2574.
44. X. Feng, L. Liu, S. Wang, and D. Zhu, *Chem. Soc. Rev.*, 2010, **39**(7), 2411-2419.
45. A. Duarte, K.-Y. Pu, B. Liu, and G.C. Bazan, *Chem. Mater.*, 2010, **23**(3), 501-515.
46. F. Feng, F. He, L. An, S. Wang, Y. Li, and D. Zhu, *Adv. Mater.*, 2008, **20**(15), 2959-2964.
47. K. Li and B. Liu, *J. Mater. Chem.*, 2012, **22**(4), 1257-1264.
48. K. Li, J. Pan, S.-S. Feng, A.W. Wu, K.-Y. Pu, Y. Liu, and B. Liu, *Adv. Funct. Mater.*, 2009, **19**(22), 3535-3542.
49. K. Li, D. Ding, D. Huo, K.-Y. Pu, N.N.P. Thao, Y. Hu, Z. Li, and B. Liu, *Adv. Funct. Mater.*, 2012, **22**(15), 3107-3115.
50. J. Geng, K. Li, K.-Y. Pu, D. Ding, and B. Liu, *Small*, 2012, **8**(15), 2421-2429.
51. C. Wu, B. Bull, C. Szymanski, K. Christensen, and J. McNeill, *ACS Nano*, 2008, **2**(11), 2415-2423.

52. C. Wu and D.T. Chiu, *Angew. Chem. Int. Ed.*, 2013, **52**(11), 3086-3109.
53. C. Yang-Hsiang, M.E. Gallina, X. Zhang, I.-C. Wu, Y. Jin, W. Sun, and D.T. Chiu, *Anal. Chem.*, 2012, **84**, 9431-9438.
54. C.M. Davis, E.S. Childress, and E.J. Harbron, *J. Phys. Chem. C*, 2011, **115**, 19065-19073.
55. Y. Osakada, L. Hanson, and B. Cui, *Chem. Commun.*, 2012, **48**, 3285-3287.
56. K. Jeong, S. Park, Y.-D. Lee, C.-K. Lim, J. Kim, B.H. Chung, I.C. Kwon, C.R. Park, and S. Kim, *Adv. Mater.*, 2013, DOI: 10.1002/adma.201301901.
57. J. Liu, D. Ding, J. Geng, and B. Liu, *Polym. Chem.*, 2012, **3**(6), 1567-1575.
58. Y. Li, J. Liu, B. Liu, and N. Tomczak, *Nanoscale*, 2012, **4**(18), 5694-5702.
59. K. Li, Y. Jiang, D. Ding, X. Zhang, Y. Liu, J. Hua, S.-S. Feng, and B. Liu, *Chem. Commun.*, 2011, **47**(26), 7323-7325.
60. D. Hühn, K. Kantner, C. Geudel, S. Brandholt, I. D. Cock, S. J. H. Soenen, P. Rivera_Gil, J.-M. Montenegro, K. Braeckmans, K. Müllen, G. U. Nienhaus, M. Klapper, and W. J. Parak, *ACS Nano*, 2013, 7(4), 3253-3263.
61. K. Lee, H. Lee, K. H. Bae, and T. G. Park, Biomaterials, 2010, **31**(25), 6530-6536.
62. S.-D. Li, and L. Huang, *Mol. Pharmaceutics*, 2008, **5**,496-504.
63. D. Ding, K. Li, Z. Zhu, K.-Y. Pu, Y. Hu, X. Jiang, and B. Liu, Nanoscale, 2011, **3**, 1997-2002.

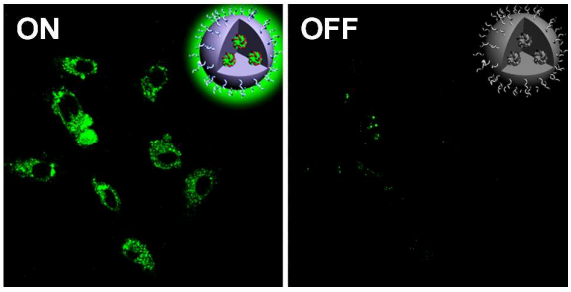

Fluorescent photoswitchable conjugated polymer nanoparticles for cell and ex vivo tumour imaging with fluorescence on/off contrast over 10-fold in tumour